Chaotic phase synchronization in small-world networks of bursting neurons

Haitao Yu, Jiang Wang, Bin Deng, Xile Wei, Y. K. Wong et al.

Citation: Chaos **21**, 013127 (2011); doi: 10.1063/1.3565027
View online: http://dx.doi.org/10.1063/1.3565027
View Table of Contents: http://chaos.aip.org/resource/1/CHAOEH/v21/i1
Published by the American Institute of Physics.

Chaotic phase synchronization in small-world networks of bursting neurons

Haitao Yu,[1] Jiang Wang,[1,a)] Bin Deng,[1] Xile Wei,[1] Y. K. Wong,[2] W. L. Chan,[2] K. M. Tsang,[2] and Ziqi Yu[3]
[1]*School of Electrical Engineering and Automation, Tianjin University, Tianjin 300072, People's Republic of China*
[2]*Department of Electrical Engineering, The Hong Kong Polytechnic University, Kowloon, Hong Kong*
[3]*School of Mechanical Engineering, Tianjin University, Tianjin 300072, People's Republic of China*

(Received 19 December 2010; accepted 18 February 2011; published online 30 March 2011)

We investigate the chaotic phase synchronization in a system of coupled bursting neurons in small-world networks. A transition to mutual phase synchronization takes place on the bursting time scale of coupled oscillators, while on the spiking time scale, they behave asynchronously. It is shown that phase synchronization is largely facilitated by a large fraction of shortcuts, but saturates when it exceeds a critical value. We also study the external chaotic phase synchronization of bursting oscillators in the small-world network by a periodic driving signal applied to a single neuron. It is demonstrated that there exists an optimal small-world topology, resulting in the largest peak value of frequency locking interval in the parameter plane, where bursting synchronization is maintained, even with the external driving. The width of this interval increases with the driving amplitude, but decrease rapidly with the network size. We infer that the externally applied driving parameters outside the frequency locking region can effectively suppress pathologically synchronized rhythms of bursting neurons in the brain. © *2011 American Institute of Physics*.
[doi:10.1063/1.3565027]

Recently, one class of neural networks which has been intensively studied is the small-world network. The small-world property turns out to be widespread property in the biological systems—often with important dynamical consequences. Models of neural systems with small-world coupling display enhanced signal-propagation speed, computational power, and synchronizability. On the other hand, chaotic phase synchronization (CPS) is a widely investigated phenomenon in a variety of physical and biological systems. Mutual phase synchronization in these systems is thought to play a substantial role in information processing. In this paper we investigate the effect of CPS of bursting neurons modeled by a network of coupled two-dimensional maps exhibiting the small-world property. We also analyze the external CPS of the bursting behavior in the studied network with a periodic driving signal applied to one arbitrarily taken neuron.

I. INTRODUCTION

Synchronization of coupled neurons in biological systems has been widely studied over the last few years. Classical phenomena such as mutual synchronization, entrainment and chaotic synchronization are now observed in many biological experiments and numerical simulations.[1–4] Theoretical and experimental studies suggest that synchronization in neuronal systems causes many physiological mechanisms of normal, as well as pathological, brain functions. For example, synchronization plays a crucial role in the mechanisms of information processing and information preface within different brain areas.[5] Synchronous oscillations in the sensorimotor cortex provide integration and coordination of the information needed for the motor control.[6] It is also suggested that synchronization is the origin of neurological diseases such as epilepsy[7] and Parkinson's disease.[8]

There are two basic types of neuronal firing activities, bursting and tonic spiking, observed in biological experiments. Bursting occurs when neuronal activity alternates between a quiescent state and fast repetitive spiking. Different types of bursting and their generation mechanisms have been extensively studied.[9–11] for its important role in enhancing the reliability of communications between neurons by facilitating transmitter release.[12] So far, many mathematical models have been developed to emulate this spiking-bursting behavior of neurons, ranging from differential equations[13] to discrete-time maps.[14,15] When coupled bursting neurons may exhibit different form of synchronization: Burst synchronization,[16,17] when only the envelopes of the spikes become synchronized; and complete synchronization[18] which involves also the synchronization of internal spikes. Additionally, chaotic phase synchronization (CPS) is another widely studied phenomenon in a verity of physical and biological systems, which is defined as the coincidence of the characteristic time scales of the interacting systems, bursting in our case, while the amplitudes remain uncorrelated.[19] During the last decade CPS in small and large neural ensembles has been studied in much detail. For a global-coupling[20] or scale-free network,[21,22] the transition to mutual CPS in bursting neurons occurs as the coupling strength is large enough.

As for a neural network, the interplay between the intrinsic dynamics of the constituent neurons and their complex pattern of connectivity strongly affects the synchronization

a)Electronic mail: jiangwang@tju.edu.cn.

dynamics of the resulting system. Recently, one class of neural networks which has been intensively studied is the small-world network,[23] which is characterized by a small value of normalized path length (just like a random network) while retaining a comparatively large value of clustering coefficient, as it occurs for a regular network. The small-world property turns out to be widespread in biological systems,[24–32] often with important dynamical consequences.[33–38] In the human functional network described by Chialvo *et al.*,[25,26] the shortest path length was found to be $L=6.0$, with a cluster coefficient of $C=0.15$, which would take the values $L=6.0$ and $C=0.00089$ if the network were to be treated as a random graph. Such network exhibits the so-called small-word property. The observation of excitatory traveling waves in the brain cortex implies that a salient feature of the circuitry is the coexistence of shortcuts and regular local connection characteristics of the small-world networks.[27–29] Experimental evidence also suggested that a small-world topology might be a general organization principle of the human brain.[30] Humphries *et al.* argue that the medial reticular formation of the brainstem is characterized by a neural network exhibiting small-world properties.[31] Moreover, a recent study using functional magnetic resonance imaging suggests that connectivity graphs formed out of cortical and sub-cortical voxels also show small-world properties.[32] Models of neural systems with small-world coupling display enhanced signal-propagation speed, computational power, and synchronizability.[33,34] Small-world networks of coupled phase oscillators synchronize almost as readily as in the mean-field model,[35–37] which may be relevant to the observed synchronization of widely separated neurons in the visual cortex.[38]

In this paper we study the CPS of bursting neurons modeled by a network of coupled two-dimensional maps[15] exhibiting the small-world property. The map-based model proposed by Rulkov *et al.*,[14,15] despite its intrinsic simplicity and low dimensionality, can reproduce characteristic behaviors of biological neurons,[14,39,40] but at essentially lower computational costs; thus allowing detailed analysis of the dynamics of large ensembles.[41–43] We investigate the parameter regimes for which chaotic bursting synchronization occurs, and the transition to phase synchronization with the variation of coupling parameters. Moreover, a periodic external driving is introduced to a single neuron of the network, thus acting as a pacemaker trying to impose its rhythm on the whole ensemble. The crucial role of the pacemaker on the dynamics of complex networks has been studied extensively.[44–47] It was shown that the periodic pacemaker can largely enhance noise-induced synchrony,[44] stochastic resonance,[45,46] and subthreshold signal detection in excitable networks.[47] Here, it is used as an electrical stimulation of the brain to suppress the undesirable synchronous rhythms related to neurological diseases, such as epilepsy and Parkinson's disease.

The remainder of this paper is organized as follows: In Sec. II, we present the map-based neuron model proposed by Rulkov and the definition of the geometrical phase of the bursting dynamics. Section III describes the simplified neural network, whose connection architecture displays the small-world property and investigates its transition to CPS with the variation of coupling parameters. In Sec. IV, we analyze the effect of external CPS of the bursting behavior in the studied networks with a periodic driving signal applied to one arbitrarily taken neuron. Finally, a brief conclusion of this paper is given in Sec. V.

II. NEURON DYNAMICS AND PHASE SYNCHRONIZATION

The single map-based neuron model proposed by Rulkov[15] can be written in the form

$$x_{n+1} = a/(1+x_n^2) + y_n, \tag{1}$$

$$y_{n+1} = y_n - \sigma x_n - \beta, \tag{2}$$

where x_n is the fast dynamical variable representing the transmembrane voltage of the neuron and y_n is the slow dynamical variable denoting the slow gating process. The first variable can emulate the spiking-bursting activity of a neuron, depending on the value of the parameter a, whereas the latter variable undergoes a slow temporal evolution due to the small value of the parameters σ and β, which model the action of an external dc bias current or the synaptic inputs to the cell. If the parameter a is selected within the range [4.1 and 4.4], the fast variable x_n of the map-based neuron displays a chaotic bursting behavior, as shown in Fig. 1(a).

In order to investigate the bursting synchronization of coupled neurons, we introduce the definition of bursting phase. For map-based neuron system (1,2), we denote $\{n_k\}$ as the moment at which the kth burst starts, which is recorded when the slow variable y_n presenting nearly regular saw-teeth oscillations gets a local maximum, as shown in Fig. 1. Then the bursting phase of a neuron at the discrete time n is defined as

$$\varphi(n) = 2\pi k + 2\pi(n-n_k)/(n_{k+1}-n_k), \quad (n_k < n < n_{k+1},\ k = 1,2,...,K), \tag{3}$$

where K is the total number of bursts during the observation time and $n_{k+1}-n_k$ is the inter-burst interval. Thus, the bursting phase of the neuron φ_n increases linearly between the moments n_k and n_{k+1} at which bursts start and gains a 2π growth over each inter-burst interval. Then the bursting

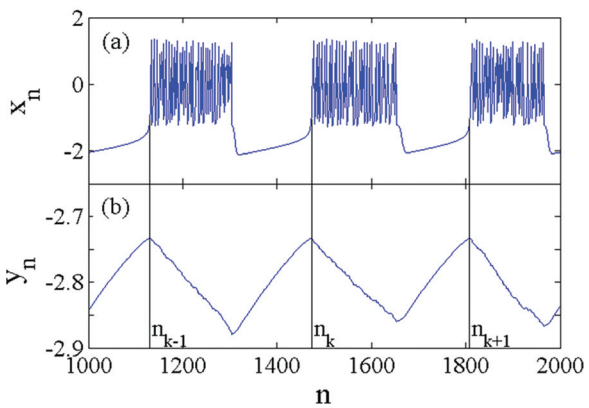

FIG. 1. (Color online) Time evolutions of the (a) fast and (b) slow variables in the map-based neuron with $\alpha = 4.1$, $\beta = \sigma = 0.001$.

frequency of a neuron can be defined as an average speed of the phase increase,

$$\Omega = \lim_{n\to\infty} (\varphi(n) - \varphi(0))/n. \quad (4)$$

For an ensemble of uncoupled neurons, they may burst at different times in a noncoherent fashion. But when they are coupled through synapses, though not exhibit a complete synchronization in the spiking time scale, yet can present a coherent behavior, since their bursting phase can synchronize through the interaction provided by the coupling term. In the case of only two coupled neurons, phase synchronization between them would indicate that their phase is approximately equal, that is, $|\varphi^{(1)} - \varphi^{(2)}| \ll 1$. But for a large number of coupled neurons, other diagnostics of phase synchronization need to be used like order parameter.

III. CHAOTIC PHASE SYNCHRONIZATION IN SMALL-WORLD NETWORKS

A. Small-world networks

In this section, we consider a network of diffusively coupled excitable neurons with small-world topology. The temporal evolution of the ith unit is described by the following set of discrete equations:

$$x_{i,n+1} = a_i/(1 + x_{i,n}^2) + y_{i,n} + I_{i,n}^{\text{syn}}(x_{i,n}), \quad (5)$$

$$y_{i,n+1} = y_{i,n} - \sigma_i x_{i,n} - \beta_i, \quad (6)$$

where $x_{i,n}$ and $y_{i,n}$ represent the fast and slow dynamical variable of the ith neuron, respectively. $I_{i,n}^{\text{syn}}(x_{i,n})$ is the coupling term, the form of which depends on the network topology chosen to describe the neural network. The coupling between the neurons may occur via two different types of synapses: The electrical and chemical ones. But for a commonly investigated model of neural network, global-coupling network, the coupling term usually considers the mean field produced by all the neurons,[20]

$$I_{i,n}^{\text{syn}}(x_{i,n}) = \varepsilon/N \sum_{j=1}^{N} x_{j,n}, \quad (7)$$

where N is the number of neurons in the ensemble, and ε is the strength of regular coupling between the given unit and the set of its "neighbors." This form of mean-field coupling has been extensively used in the studies on synchronization of bursting neurons.[20,48] However, such a model exhibits regular connection topology only, in which each neuron is connected with all other neurons of the ensemble. Considering the nonuniform connectivity of realistic neural networks in the small-world network we use the coupling term of the form[21,22,49]

$$I_{i,n}^{\text{syn}}(x_{i,n}) = \varepsilon/k_i \sum_{j\in M} x_{j,n}, \quad (8)$$

where ε is the strength of the coupling, and we assumed that each unit i is connected with a set M comprising k_i; other units are randomly chosen along the network.

To construct a small-world network, we consider following the random rewiring procedure proposed by Watts and Strogatz.[23] Staring from a ringlike network with regular connectivity, where each node is connected to its λ, nearest neighbors on each side of the ring, we rewire each edge at random with the probability p. By increasing the probability p the architecture of the network is tuned between two extremes, regular ($p = 0$) and random ($p = 1$) networks. Small-world networks are characterized by intermediate value of the probability $0 < p < 1$, as exemplified in Fig. 2. These networks has a small value of characteristic path length L, comparable with that of a random network, while get a large value of clustering coefficient C, just like a regular network. The shortest path length is defined as the average number of edges in the shortest path between any two vertices; and the clustering coefficient is the fraction of edges between the neighbors with respect to maximum possible.[23]

In the following we consider a small-world network containing $N = 1000$ map-based neurons, which is obtained from a regular ring ($\lambda = 10$) with different values of rewiring probability p. In view of the diversity of neurons in the real biological system, we set a_i as random and uniformly distributed in [4.1 and 4.4] and $\sigma_i = \beta_i = 0.001$, so that each uncoupled neuron produces chaotic bursts.

B. Phase synchronization of bursting neurons

In what follows, we will systematically analyze the effects of different coupling strength ε and rewiring probability p on the CPS of the small-world network. Here, we do not expect synchronization in the spiking time scale, but we seek a weaker form of synchronization in the bursting time

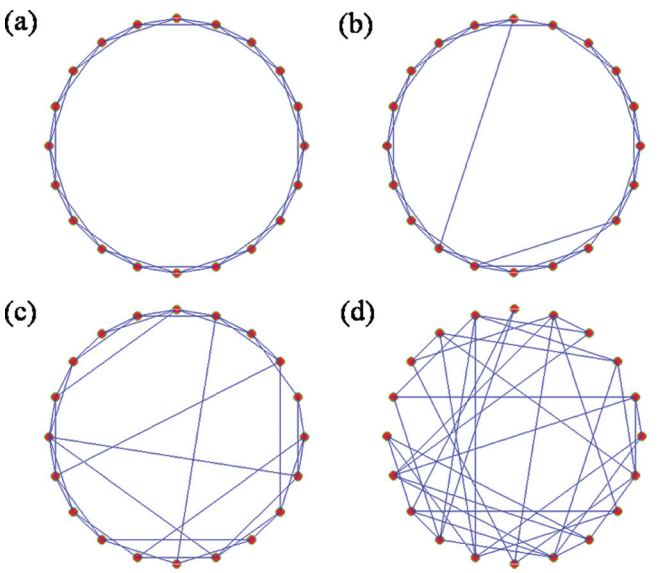

FIG. 2. (Color online) Example of considered small-world network topologies. Given 20 isolated nodes. (a) Regular ringlike network characterized by $p = 0$. Each node is connected to its $\lambda = 2$ nearest neighbors on each side of the ring. Realization of small-world topology via different random rewiring probability: (b) $p = 0.05$ and (c) $p = 0.2$. (d) Realization of random network via random rewiring probability $p = 1$.

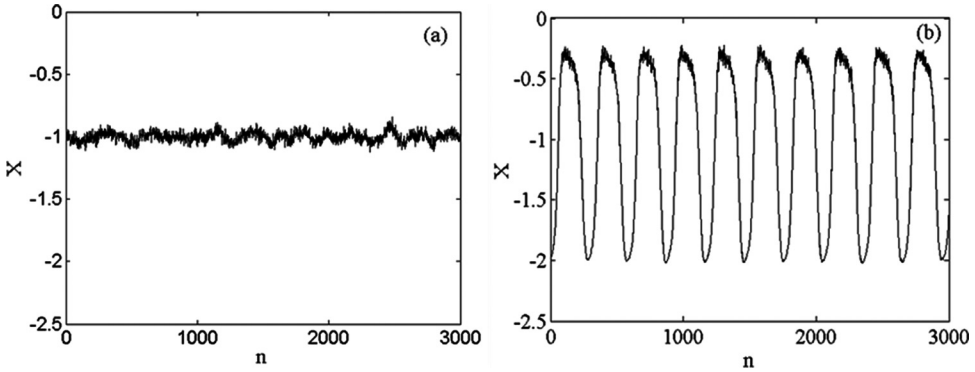

FIG. 3. The mean field of (a) an uncoupled ($\varepsilon = 0$) and (b) a strongly coupled ($\varepsilon = 0.05$) small-world network with size $N = 1000$ and rewiring probability $p = 0.2$.

scale. One useful diagnostic of synchronization, the mean field of the ensemble, is used which is defined as

$$X_n = 1/N \sum_{j=1}^{N} x_{j,n}. \tag{9}$$

In Fig. 3, a transition to CPS is observed as the coupling strength between the neurons increases. The typical time evolutions of uncoupled and synchronized bursting neurons are given in Fig. 4. When the neurons are uncoupled ($\varepsilon = 0$), they burst at different times in a noncoherent fashion [Figs. 4(a) and 4(c)] and the mean field fluctuates randomly with a small amplitude, Fig. 3(a). Alternatively, when the coupling strength between the neurons is large enough ($\varepsilon = 0.05$), a large amplitude mean field is formed [Fig. 3(b)] and its quasi-periodic oscillations make neurons to develop a common rhythm [Figs. 4(b) and 4(d)]. Notably, only on the slow time scale dynamics become coherent as the neurons are bursting synchronously, and the fast time scale spiking remains uncorrelated, but this does not substantially contribute to the mean-field dynamics, which is close to periodic.

Since a state of synchronized bursting in the small-world network is characterized by a large-amplitude oscillation of a macroscopic mean field, whereas small-amplitude noisy fluctuations mark the absence of synchronization: A quantitative measure of synchronization is the variance of mean-field oscillation $\mathrm{Var}(X)$. Figure 5 depicts the values of this variance versus the coupling strength ε for different values of p. Obviously, the synchronization of bursts exhibits strong dependence on the rewiring probability. In particular, the network only gets weak synchronization in the absence of shortcuts. But when a tiny fraction of the shortcuts are introduced into the system, on the other hand, the dynamics of the system changes dramatically, undergoing a transition to CPS at a critical value ε_c (compare curves for $p = 0$ and for $p = 0.05$ in Fig. 5). Above the transition threshold bursting synchronization is achieved and the mean field of the whole network shows large-amplitude oscillations, while below the threshold the coupling is not strong enough to yield a synchronized rhythm and the mean field exhibits irregular oscillations of small amplitude due to the finite size of the network (depending on $1/N$ with the number N of oscillators). Remarkably, the critical value ε_c decreases with the increase of rewiring probability p. This is because in the small-world networks there are more shortcuts which allow

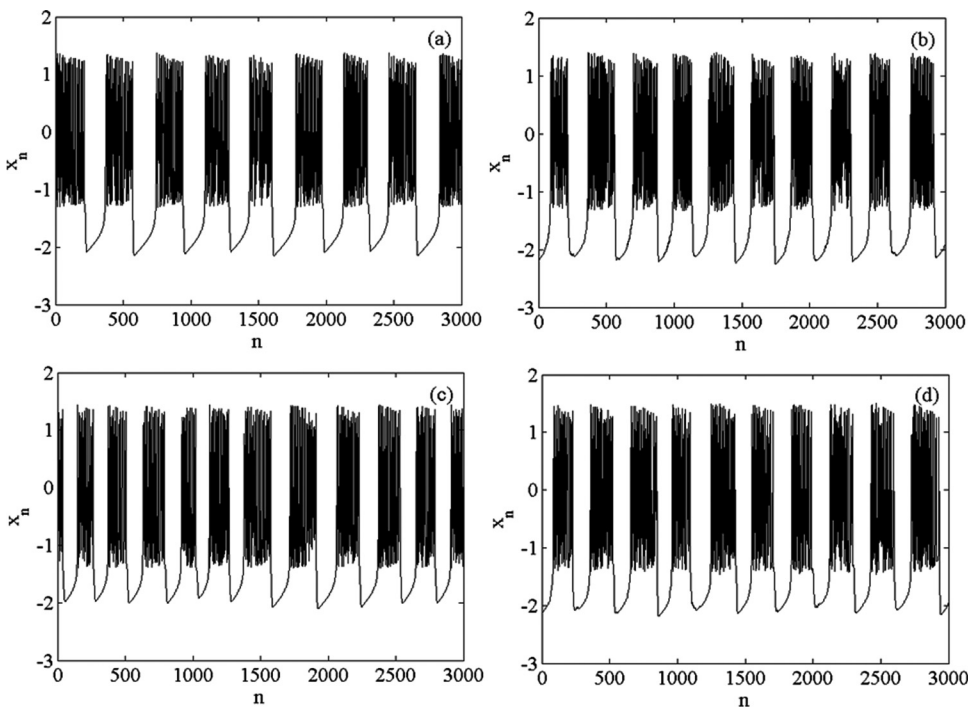

FIG. 4. Time evolutions of the fast variable for two selected neurons ($\alpha_1 = 4.1$ and $\alpha_2 = 4.2$) for the small-world network with $\varepsilon = 0$ [(a) and (c)] and $\varepsilon = 0.05$ [(b) and (d)].

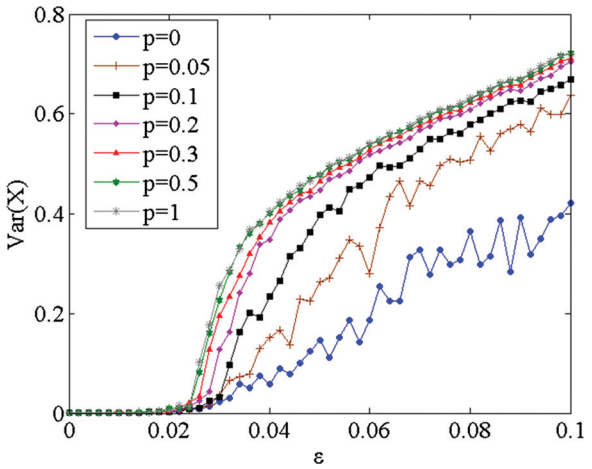

FIG. 5. (Color online) The variance of the mean-field oscillation Var(X) versus the coupling strength ε for different values of rewiring probability p in the small-world network with size $N = 1000$.

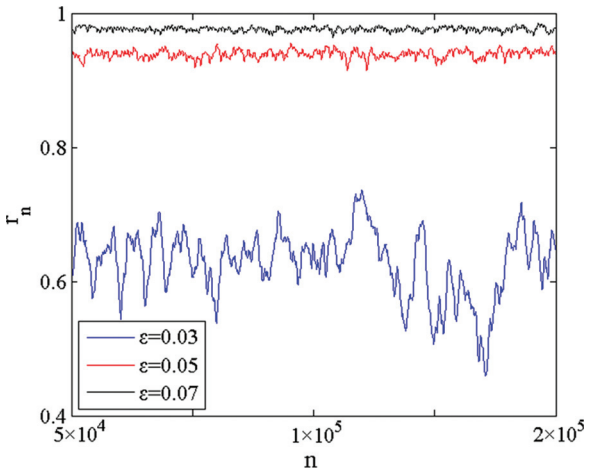

FIG. 7. (Color online) Time evolutions of the order parameter r for different values of coupling strength ε in the small-world network with size $N = 1000$ and rewiring probability $p = 0.2$.

the neural activity to spread across the network more quickly. In fact, for sparsely connected networks in general, rhythms are more robust when the topology architecture of the network is random as opposed to structured. Moreover, as p grows, bursting synchronization, measured by Var(X) in Fig. 5, saturates and does not show significant difference for $p > p_c \approx 0.5$. It is thus indicated that phase synchronization is almost the same as that for $p = 1$ and can be achieved with relatively small amount of shortcuts $p = 0.5$. Similar results were obtained for a small-world network of coupled phase oscillators.[35]

If the neuron phases are synchronized, so are their bursting frequencies. Hence, we can compare the bursting frequencies Ω_i of the neurons in the small-world network with those frequencies at zero-coupling $\Omega_{0,i}$, which fluctuate randomly among all sites. As shown in Fig. 6, when the coupling strength ε is low enough, there is no phase synchronization and a linear dependence between Ω_i and $\Omega_{0,i}$ is observed. Increasing the coupling strength leads to the appearance of synchronization plateaus which gradually increase in size. When the coupling strength exceeds the threshold ε_c, the frequencies of all coupled neurons are distributed around a mean value, implying that phase and frequency synchronization of the bursts is achieved.

We can also use another diagnostic of CPS, which is the asymptotic behavior of the order parameter[20]

$$r = \lim_{n\to\infty} \left| \sum_{k=1}^{N} e^{i\varphi(k,n)} \right|. \tag{10}$$

As shown in Fig. 7, for weakly coupled ($\varepsilon = 0.03$) ensemble of neurons, the burst phases $\varphi(k,n)$ are spatially uncorrelated such that the order parameter r fluctuate around a small value ($\sim$0.6) and with much dispersion. Alternatively, in a completely phase synchronized state ($\varepsilon = 0.07$) the phases $\varphi(k,n)$ are approximately equal, resulting that the order parameter r tends to unity. Thus, we can use this order parameter to investigate the transition to phase synchronization of bursts as the coupled strength is varied, as shown in Figs. 8 and 9. As one can see, the order parameter r indeed undergoes a transition to coherence at the critical value ε_c, just like

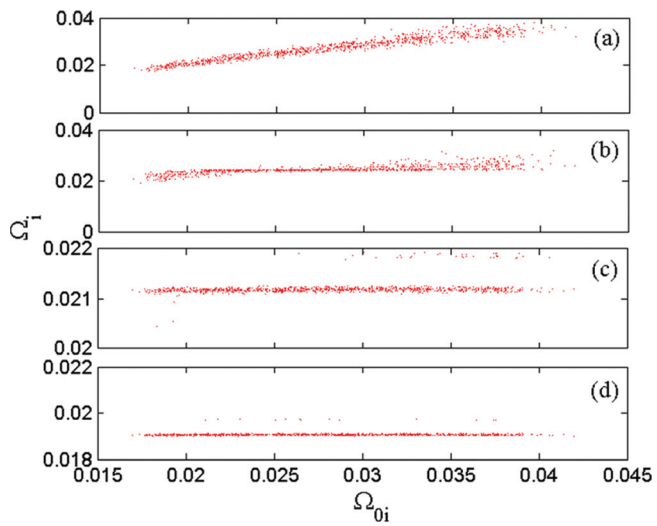

FIG. 6. (Color online) Bursting frequencies for the small-world network versus those at zero-coupling. (a) $\varepsilon = 0.2$, (b) $\varepsilon = 0.32$, (c) $\varepsilon = 0.5$, and (d) $\varepsilon = 0.7$.

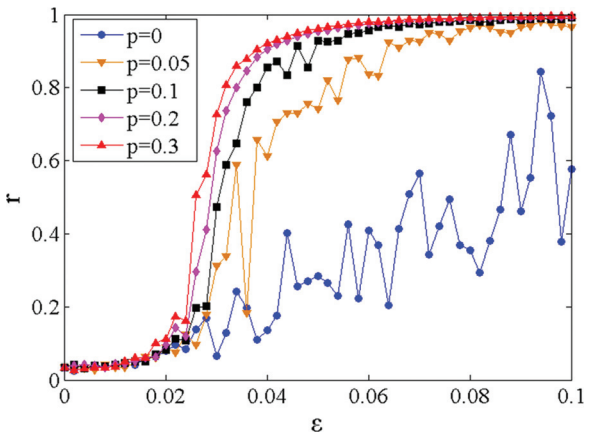

FIG. 8. (Color online) The order parameter r as a function of the coupling strength ε for different values of rewiring probability p in the small-world network with size $N = 1000$.

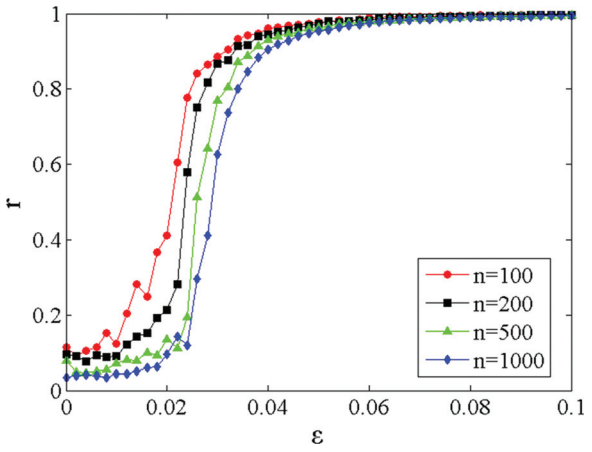

FIG. 9. (Color online) The order parameter r as a function of the coupling strength ε for different values of network size with rewiring probability $p = 0.2$.

the behavior of mean-field variance. Its minimum is obtained for zero-coupling and decreases as the network size turns larger (depending on $1/N$ with the number N of oscillators). Moreover, the critical value ε_c decreases as the rewiring probability p is gradually increased (Fig. 8), whereas increases with the enlargement of the network size (Fig. 9).

IV. EXTERNAL CHAOTIC PHASE SYNCHRONIZATION

By now, we have demonstrated that a small-word neural network can get well-coordinated synchronization with a relative large value of coupling parameter. However, synchronization is not always desirable. In fact, pathologically strong synchronization processes may severely impair brain function. For example, many neurological diseases, such as epilepsy and Parkinson's disease, are suggested to be caused by a strong synchronized population of oscillatory neurons in the cortical and thalamic areas.[50,51] Hence, suppression of such undesirable synchronized behavior of the neuron population has become a challenging problem of neuroscience. Here, we consider the possibility to control such rhythm (often pathological) by means of external periodic driving signal. Such technique has been extensively studied in deep brain stimulation (DBS), where strong high-frequency (>100 Hz) electrical pulse-train stimulation is permanently administered to sub-cortical target areas to block the synchronized neural activity.[52,53] In this work, however, we would like to investigate the parameter regions where external CPS occurs, which is regarded as an inverse problem of synchronization suppression.

We apply a periodic signal $d\sin(wn)$ to one arbitrarily taken neuron i^* so that its fast variable x has the following equation:

$$x_{i^*,n+1} = a_{i^*}/(1 + x_{i^*,n}^2) + y_{i^*,n} + I_{i^*,n}^{\mathrm{syn}}(x_{i^*,n}) + d\sin(wn). \tag{11}$$

The equation for the slow variable of neuron i^* and those for other $N-1$ neurons remains unchanged. The number of bursting neurons in the studied network is $N = 100$. In order to investigate the effect of the external driving signal, we fix

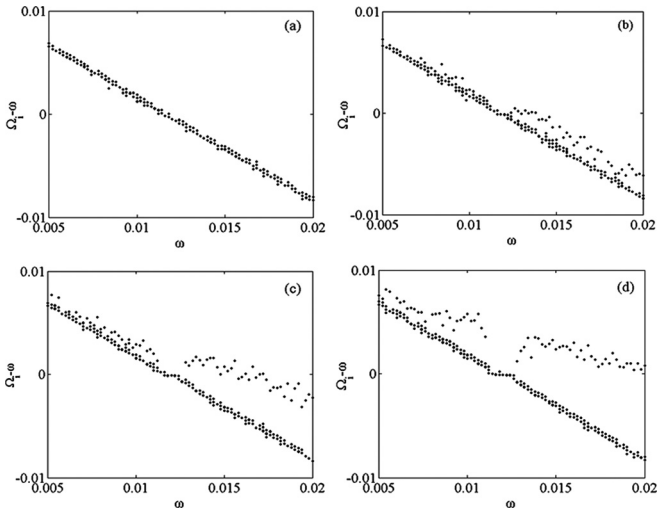

FIG. 10. The frequency difference between bursting neurons and external driving signal versus the external driving frequency for the small-world network with coupling strength $\varepsilon = 0.2$ and a driving signal with amplitude (a) $d = 0.05$, (b) $d = 0.1$, (c) $d = 0.15$, and (d) $d = 0.2$.

the coupling strength value $\varepsilon = 0.2$, so that the unperturbed ensemble ($d = 0$) exhibits bursting synchronization and their corresponding frequencies Ω_i lock approximately at a common value.

With the variation of the frequency ω of the driving signal for different values of signal amplitude d, we observe the effect of external frequency locking of bursts (i.e., external CPS). As shown in Fig. 10, the frequency mismatch $\Omega_i - \omega$ is plotted against ω for all neurons which belong to the network. Obviously, when the signal amplitude is too small [Fig. 10(a)], the difference $\Omega_i - \omega$ vanishes for a particular value of ω. But for $d \geq 0.1$ a narrow frequency locking region is obtained around $\omega = 0.012$ [Fig. 10(b)], where $\Omega_i - \omega = 0$ is satisfied. The width of this frequency locking interval, $\Delta\omega$, increases with the signal amplitude in the direction of higher frequencies of the driving [Figs. 10(c) and 10(d)]. However, for $d > \varepsilon$, a further increase in the amplitude of driving force does not enlarge the frequency locking interval significantly [Fig. 12(a)]. In fact, this widening trend is limited by the intensity of the driving signal, since for

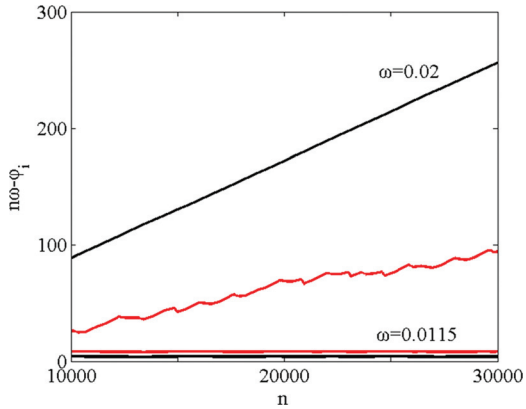

FIG. 11. (Color online) Time evolutions of difference between bursting phase and driving phase for different values of driving frequency. The red line corresponds to the driven neuron, and the black line corresponds to other mutually synchronized neurons.

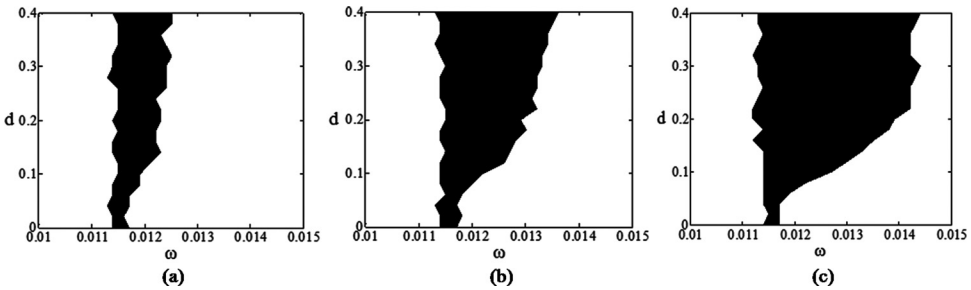

FIG. 12. The frequency locking tongue in the parameter plane amplitude against frequency of the external driving signal for different number of driven neurons: (a) $N_{dr}= 1$, (b) $N_{dr}= 2$, and (c) $N_{dr}= 4$.

relatively large amplitudes of driving signal outside the synchronization region, i.e., the driving frequency is higher than the upper end of the frequency locking interval, the driven neuron switches to a frequency different from those of driving signal and of other mutually synchronized oscillators.

In order to investigate the effect of driving frequencies inside and outside the external CPS region, we plot in Fig. 11 the time evolution of phase difference between the bursting phase $\varphi(n)$ and the driving phase $\phi \equiv \omega n$. For a frequency ω within the frequency locking interval, $\omega = 0.0115$, the difference keeps constant and is very small for all neurons. But for a frequency ω outside the frequency locking interval, $\omega = 0.02$, there is an overall linearly increasing trend of the phase difference with evolution time, indicating that the corresponding frequencies are different from the external driving. In this situation, the influence of the external signal is strong enough to steer the system out of phase synchronization state, leading to a phase drift.

The frequency locking interval shown in Fig. 10 is actually a cross section of the Arnold-like tongue in the parameter plane amplitude against the frequency of the external driving signal, Fig. 12(a). This tonguelike structure characterizes a region where chaotic bursting synchronization is maintained, even with the external driving. Hence the desirable choices for suppressing synchronization would be those outside this tongue. Notice that the synchronization tongue obtained in Fig. 12 is greatly asymmetric, since the unperturbed frequency ω_0 is not located at the middle of the frequency locking interval, especially for large driving amplitudes. A detailed explanation for this asymmetry of the frequency locking tongue has been provided by Ivanchenko *et al.*[20] An imposed periodic signal precipitates a burst of a neuron into a quiescent regime when positive and delays it when negative. If the external driving frequency is higher than that of the mutual synchronized network, the periodic signal will fasten the oscillations of the driven neuron. When the driven neuron starts bursting, the abrupt change of its amplitude increases the mean field perceived by all other neurons, pushing them toward bursting. Hence, a higher frequency would give better synchronization effect. On the contrary, if the frequency of external driving signal is smaller than that of the synchronized ensemble, only tiny synchronization effect can be expected. Hence, a local driving can result in external CPS of the whole network only when the oscillations in the unperturbed network ($d = 0$) are mutually synchronized.

To gain more insights into the dependence of external CPS of the small-world network on p and ε, in Fig. 13 we plot the width of frequency locking interval $\Delta\omega$ as a function of rewiring probability p for different coupling strength ε, with a fixed driving amplitude d. Evidently, $\Delta\omega$ exhibits a resonancelike behavior with respect to p, thus indicating the existence of an optimal small-world topology for the external CPS of the network. Similar results were also obtained from the study of stochastic resonance on excitable small-world networks.[45,46] Since the effectiveness of the pacemaker to enforce its rhythm to other units in the network relies on specific topology properties of the network, such as the normalized clustering coefficient C and the characteristic path length L, Perc has proposed the ratio $R = C/L$ as a crucial quantity defining the optimal properties of a network to facilitate the spreading of the localized pacemaker-emitted rhythmic activity.[45] It has been proved that there exists a peak value of R obtained by some value of p, which may just warrant the largest peak value of $\Delta\omega$ in our work. From Fig. 13 we can also find that the value of p which gives the maximal $\Delta\omega$ decreases when the coupling strength increases. Thus, as the coupling increases the peak $\Delta\omega$ is obtained for fewer added shortcuts, or equivalently, by a lower value of p. Moreover, the maximal $\Delta\omega$ decreases as the coupling strength increases; however, stronger coupling strength contributes to a higher value of $\Delta\omega$ in regular network (in the limit $p \to 0$).

Finally, we study the effect of network size on the external CPS of small-world networks. As shown in Fig. 14, the width of frequency locking interval $\Delta\omega$ decreases as the number of oscillators in the ensemble grows, implying that the external CPS becomes too difficult for large networks.

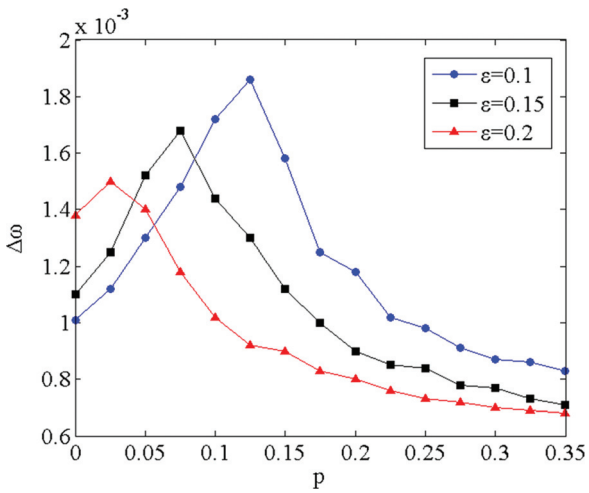

FIG. 13. (Color online) Width of the frequency locking interval $\Delta\omega$ versus the rewiring probability p for different values of coupling strength: $\varepsilon = 0.1$ (blue circles), $\varepsilon = 0.15$ (black squares), and $p = 0.2$ (red triangles). The fixed driving amplitude is $d = 0.2$.

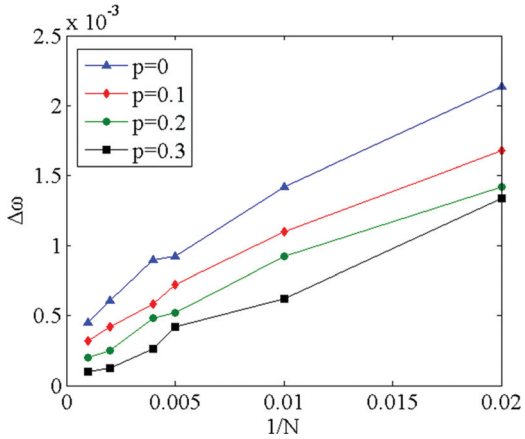

FIG. 14. (Color online) Width of the frequency locking interval $\Delta\omega$ versus the inverse number of neurons in the network $1/N$ for different rewiring probability: $p = 0$ (blue triangles), $p = 0.1$ (red diamonds), $p = 0.2$ (green circles), and $p = 0.3$ (black squares). The fixed coupling strength is $\varepsilon = 0.2$ and driving amplitude $d = 0.2$.

Similar results were also obtained for global-coupling and scale-free neural networks.[20–22] This is because the contribution of the driven oscillator to the mean field is proportional to ε/N. One possible way to overcome this problem is to apply the same driving signal not to one, but to several arbitrarily chosen neurons at the same time. As shown in Fig. 15 increasing the number of driving will enlarge the width of frequency locking tongue (also see Fig. 10 for details).

V. CONCLUSIONS

In conclusion, we have investigated the CPS in a system of coupled map-based neurons in small-world networks. A transition to mutual phase synchronization has been observed as the coupling strength exceeds a threshold. This transition occurs on the time scale of bursting, while on the time scale of spiking, the synchrony does not appear. We have seen that phase synchronization is largely facilitated by a large fraction p of shortcuts and saturates for $p > 0.5$, indicating that the same synchronizability as the random network can be achieved with relatively small number of shortcuts.

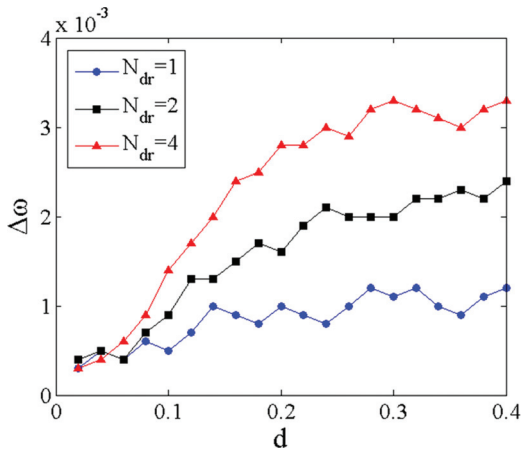

FIG. 15. (Color online) Width of the frequency locking interval $\Delta\omega$ versus the driving amplitude d for different number of driven neurons: $N_{dr} = 1$ (blue circles), $N_{dr} = 2$ (black squares), and $N_{dr} = 4$ (red triangles).

We have also analyzed the external CPS in the small-world networks by a periodic external signal applied to one arbitrarily taken neuron. We have shown frequency locking tongues in the driving parameter space, representing parameters values for which synchronization is maintained, even with the external driving. Since many neurological diseases are suggested to be related with strong synchronized oscillations of bursting neurons, we infer that effective synchronization suppression can be realized with the driving parameters outside these synchronization tongues. It is worth noting that the width of these synchronization tongues depends extensively on coupling strength and rewiring probability. In particular, there exists an optimal small-world topology, warranting the largest peak value of the frequency locking interval. Moreover, their widths increase with the driving amplitude, but decrease rapidly with the network size. On the other hand, increasing the number of driving neuron will enlarge the width of frequency locking tongue, a factor that should be considered in practical intervention experiments.

ACKNOWLEDGMENTS

This work was supported by the National Natural Science Foundation of China (Grant No. 61072012), the Young Scientists Fund of the National Natural Science Foundation of China (Grant Nos. 50707020, 60901035, and 50907044), and the Hong Kong Polytechnic University (Grant No. G-U488).

[1]N. V. Manyakov and M. M. Van Hulle, Chaos **18**, 037130 (2008).
[2]R. C. Elson, A. I. Selverston, R. Huerta, N. F. Rulkov, M. I. Rabinovich, and H. D. I. Abarbanel, Phys. Rev. Lett. **81**, 5692 (1998).
[3]A. K. Kryukov, V. S. Petrov, L. S. Averyanova, G. V. Osipov, W. Chen, O. Drugova, and C. K. Chan, Chaos **18**, 037129 (2008).
[4]S. Boccaletti, J. Kurths, G. Osipov, D. L. Valladares, and C. S. Zhou, Phys. Rep. **366**, 1 (2002).
[5]W. Singer, Annu. Rev. Physiol. **55**, 349 (1993).
[6]W. A. MacKay, Trends Cogn. Sci. **1**, 176 (1997).
[7]H. J. Freund, Physiol. Rev. **63**, 387 (1983), http://physrev.physiology.org/content/63/2/387.extract.
[8]R. Levy, W. D. Hutchison, A. M. Lozano, and J. O. Dostrovsky, J. Neurosci. **20**, 7766 (2000), http://www.jneurosci.org/content/20/20/7766.short.
[9]E. M. Izhikevich, Int. J. Bifurcation Chaos **10**, 1171 (2000).
[10]E. M. Izhikevich and F. C. Hoppensteadt, Int. J. Bifurcation Chaos **14**, 3847 (2004).
[11]A. L. Shilnikov and N. F. Rulkov, Int. J. Bifurcation Chaos **13**, 3325 (2003).
[12]J. E. Lisman, Trends Neurosci. **20**, 38 (1997).
[13]A. L. Hodgkin and A. F. Huxley, J. Physiol. **117**, 500 (1952), http://www.ncbi.nlm.nih.gov/pmc/articles/PMC1392413/.
[14]N. F. Rulkov, Phys. Rev. E **65**, 041922 (2002).
[15]N. F. Rulkov, Phys. Rev. Lett. **86**, 183 (2001).
[16]G. Tanaka, B. Ibarz, M. A. Sanjuan, and K. Aihara, Chaos **16**, 013113 (2006).
[17]X. Shi and Q. Lu, Physica A **388**, 2410 (2009).
[18]X. Shi and Q. Lu, Chin. Phys. **14**, 77 (2005).
[19]M. G. Rosenblum, A. S. Pikovsky, and J. Kurths, Phys. Rev. Lett. **76**, 1804 (1996).
[20]M. V. Ivanchenko, G. V. Osipov, V. D. Shalfeev, and J. Kurths, Phys. Rev. Lett. **93**, 134101 (2004).
[21]C. A. S. Batista, A. M. Batista, J. A. C. de Pontes, R. L. Viana, and S. R. Lopes, Phys. Rev. E **76**, 016218 (2007).
[22]C. A. S. Batista, A. M. Batista, J. A. C. de Pontes, S. R. Lopes, and R. L. Viana, Chaos, Solitons Fractals **41**, 2220 (2009).
[23]D. J. Watts and S. H. Strogatz, Nature **393**, 440 (1998).
[24]O. Shefi, I. Golding, R. Segev, E. Ben-Jacob, and A. Ayali, Phys. Rev. E **66**, 021905 (2002).
[25]D. R. Chialvo, Physica A **340**, 756 (2004).

[26]O. Sporns, D. R. Chialvo, M. Kaiser, and C. C. Hilgetag, Trends Cogn. Sci. **8**, 418 (2004).
[27]D. A. McCormick and D. Contreras, Ann. Rev. Physiol. **63**, 815 (2001).
[28]J. Y. Wu, L. Guan, and Y. Tsau, J. Neurosci. **19**, 5005 (1999), http://www.jneurosci.org/content/19/12/5005.short.
[29]M. Bazhenov, N. F. Rulkov, and I. Timofeev, J. Neurophysiol. **100**, 1562 (2008).
[30]C. J. Honey, R. Kotter, M. Breakspear, and O. Sporns, Proc. Natl. Acad. Sci. U.S.A. **104**, 10240 (2007).
[31]M. D. Humphries, K. Gurney, and T. J. Prescott, Proc. R. Soc. London B **273**, 503 (2006).
[32]M. P. Van der Heuvel, *etal*., Neuroimage **43**, 528 (2008).
[33]L. F. Lago-Fernández, R. Huerta, F. Corbacho, and J. A. Sigüenza, Phys. Rev. Lett. **84**, 2758 (2000).
[34]Q. Y. Wang, Z. S. Duan, M. Perc, and G. R. Chen, EPL **83**, 50008 (2008).
[35]H. Hong, M. Y. Choi, and B. J. Kim, Phys. Rev. E **65**, 026139 (2002).
[36]Y. Wu, Y. Shang, M. Chen, C. Zhou, and J. Kurths, Chaos **18**, 037111 (2008).
[37]A. Rothkegel and K. Lehnertz, Chaos **19**, 015109 (2009).
[38]C. M. Gray, P. König, A. K. Engel, and W. Singer, Nature **338**, 334 (1989).
[39]M. Perc, Eur. J. Phys. **27**, 451 (2006).
[40]M. Perc, Chaos, Solitons Fractals **31**, 64 (2007).
[41]Q. Wang, M. Perc, Z. Duan, and G. Chen, Phys. Rev. E **80**, 026206 (2009).
[42]Q. Wang, G. Chen, and M. Perc, PLoS ONE **6**, e15851 (2011).
[43]Q. Wang, M. Perc, Z. Duan, and G. Chen, Physica A **389**, 3299 (2010).
[44]M. Perc and M. Marhl, Phys. Lett. A **353**, 372 (2006).
[45]M. Ozer, M. Perc, and M. Uzuntarla, Phys. Lett. A **373**, 964 (2009).
[46]M. Perc, Phys. Rev. E **76**, 066203 (2007).
[47]V. Volman and M. Perc, New J. Phys. **12**, 043013 (2010).
[48]N. F. Rulkov, Phys. Rev. Lett. **86**, 183 (2001).
[49]C. A. S. Batista, S. R. Lopes, R. L. Viana, and A. M. Batista, Neural Networks **23**, 114 (2010)
[50]W. W. Albert, E. J. Wright, and B. Feinstein, Nature **221**, 670 (1969).
[51]I. Timofeev and M. Steriade, Neuroscience **123**, 299 (2004).
[52]A. L. Benabid, A. Benazzous, and P. Pollak, Mov. Disord. **17**, 73 (2002).
[53]A. L. Benabid, P. Pollak, C. Gervason, D. Hoffmann, D. M. Gao, M. Hommel, J. E. Perret, and J. de Rougemount, Lancet **337**, 403 (1991).